

## Low-activated Li-Ion Mobility and Metal to Semiconductor Transition in $\text{CdP}_2@Li$ Phases

Nadine Eckstein<sup>†</sup>, Ilona Krüger<sup>†</sup>, Frederik Bachhuber<sup>‡</sup>, Richard Wehrich<sup>‡</sup>, Jose Enrique Barquera-Lozada<sup>§</sup>, Leo van Wüllen<sup>§</sup>, Tom Nilges<sup>\*,†</sup>

### Supporting Information

#### Table of contents

1. X-ray structure data of  $\text{Li}_{0.2}\text{CdP}_2$  and  $\alpha'$ - $\text{CdP}_2$
2. Verification of ICP results on  $\text{Li}_{0.2}\text{CdP}_2$  and  $\alpha'$ - $\text{CdP}_2$
3. Analysis of the de-lithiation product of  $\text{Li}_{0.2}\text{CdP}_2$
4. DSC-analysis of  $\text{Li}_{0.2}\text{CdP}_2$
5. Conductivity measurements of  $\text{Li}_{0.2}\text{CdP}_2$  and  $\alpha'$ - $\text{CdP}_2$
6. Quantum chemical calculations of  $\text{Li}_{0.2}\text{CdP}_2$  and polymorphic  $\text{CdP}_2$
7. Quantification of proton content with  $^1\text{H}$ -MAS-NMR in  $\alpha'$ - $\text{CdP}_2$

1. X-ray structure data of  $\text{Li}_{0.2}\text{CdP}_2$  and  $\alpha'$ - $\text{CdP}_2$

Data from X-ray single crystal and powder experiments are summarized in Table SII.

**Table SII.** Crystallographic data of  $\text{Li}_{0.2}\text{CdP}_2$  and  $\alpha'$ - $\text{CdP}_2$ , derived from single crystal and powder data.

compound	$\text{Li}_{0.2}\text{CdP}_2$	$\text{Li}_{0.2}\text{CdP}_2$	$\text{Li}_{0.2}\text{CdP}_2$	$\alpha'$ - $\text{CdP}_2$	$\alpha'$ - $\text{CdP}_2$
refined composition	$\text{CdP}_2$	$\text{CdP}_2$	$\text{CdP}_2$	$\text{CdP}_2$	$\text{CdP}_2$
method	single crystal	single crystal	powder sample	single crystal	powder sample
temperature (K)	123(2)	293(2)	293(5)	293(5)	293(5)
molar mass ( $\text{g mol}^{-1}$ )	174.4	174.4	174.4	174.4	174.4
crystal size ( $\text{mm}^3$ )	0.1x0.1x1.4	0.1x0.1x1.4	-	0.1x0.1x0.9	-
crystal color	black	black	black	black	Black
crystal system	tetragonal	tetragonal	tetragonal	tetragonal	tetragonal
space group	$I 4_122$	$I 4_122$	$I 4_122$	$I 4_122$	$I 4_122$
lattice parameters		taken from powder data		taken from powder data	
$a$ ( $\text{\AA}$ )	7.6508(5)	7.6691(8)	7.6691(8)	7.6829(2)	7.6829(2)
$c$ ( $\text{\AA}$ )	4.4421(2)	4.4467(4)	4.4467(4)	4.46036(11)	4.46036(11)
$V$ ( $\text{\AA}^3$ )	260.02(3)	261.53(4)	261.53(4)	263.279(12)	263.279(12)
$Z$	4	4	4	4	4
$\rho_{\text{calc}}$ ( $\text{g cm}^{-3}$ )	4.45*	4.43*	4.43*	4.40	4.40
diffractometer	BRUKER APEX	BRUKER APEX	STOE STADI P	OXFORD EXC.	STOE STADI P
radiation	Mo-K $\alpha$ (0.71069 $\text{\AA}$ )	Mo-K $\alpha$ (0.71069 $\text{\AA}$ )	Cu-K $\alpha 1$ (1.54051 $\text{\AA}$ )	Mo-K $\alpha$ (0.71069 $\text{\AA}$ )	Cu-K $\alpha 1$ (1.54051 $\text{\AA}$ )
monochromator	graphite	graphite	germanium	graphite	germanium
absorption correction	numerical	numerical	none	numerical	none
independent reflections	571	517		118	
$R_{\text{int}}$ (all)	2.77	2.26		1.99	
$R_p$			2.04		2.62
refinement	least-squares on $F^2$	least-squares on $F^2$	least-squares on $F^2$	least-squares on $F^2$	least-squares on $F^2$
$R$ ( $I > 3\sigma_I$ )	2.98	2.23	2.84	1.60	3.92
$wR$ ( $I > 3\sigma_I$ )	7.54	4.33	2.87	4.22	4.19
$R$ (all)	3.16	3.09	2.90	1.60	4.19
$wR$ (all)	7.59	4.54	2.87	4.22	4.21
parameters	9	9	32	9	232
GOF (all)	2.57	1.25	1.65	1.92	2.453
residual electron density max/min ( $\text{e \AA}^{-3}$ )	1.32/ -1.67	0.60/ -0.63	0.66/ -0.58	0.25/ -0.53	1.36/ -1.20

\* density calculated on basis of Cd and P only

**Table SI2.** Atomic coordinates and isotropic displacement parameters for  $\text{Li}_{0.2}\text{CdP}_2$  and  $\alpha'$ - $\text{CdP}_2$  at 293 K (single crystal data) and for  $\text{Li}_{0.2}\text{CdP}_2$ . Isotropic displacement parameters were fixed in the Rietveld refinement. All positions are fully occupied.

	atom	x	y	z	$U_{\text{ani}}$
$\text{Li}_{0.2}\text{CdP}_2$ , 123K	Cd1	0	0	0	0.01146(7)
	P1	0.42610(10)	1/4	1/8	0.00439(17)
$\text{Li}_{0.2}\text{CdP}_2$ , 293 K	Cd1	0	0	0	0.01609(5)
	P1	0.42541(8)	1/4	1/8	0.00989(14)
$\text{Li}_{0.2}\text{CdP}_2$ , 293 K (Rietveld data)	Cd1	0	0	0	0.025(2)
	P1	0.4246(11)	1/4	1/8	0.01
$\text{CdP}_2$ , 293 K	Cd1	0	0	0	0.0157(2)
	P1	0.42565(15)	1/4	1/8	0.0097(3)
$\text{CdP}_2$ , 293 K (Rietveld data)	Cd1	0	0	0	0.0115(5)
	P1	0.4256(6)	1/4	1/8	0.01

We have performed Rietveld analyses of  $\text{Li}_{0.2}\text{CdP}_2$  and  $\alpha'$ - $\text{CdP}_2$  using the structure models derived from single crystal data structure analyses. For profile fitting we used a Lorentzian function, and a Legendre polynomial with 17 or 13 independent parameters for background description, respectively. All isotropic displacement parameters were refined without restrictions for each individual position. The lattice parameters are  $a = 7.6691(8) \text{ \AA}$ ,  $c = 4.4467(4) \text{ \AA}$  and  $V = 261.53(4) \text{ \AA}^3$  for  $\text{Li}_{0.2}\text{CdP}_2$  (Figure 4) and  $a = 7.6829(2) \text{ \AA}$ ,  $c = 4.46036(11) \text{ \AA}$  and  $V = 263.279(12) \text{ \AA}^3$  for  $\alpha'$ - $\text{CdP}_2$ . Hence, the unit cell  $\alpha'$ - $\text{CdP}_2$  (kept in air) is bigger than for  $\text{Li}_{0.2}\text{CdP}_2$  (kept under argon). Lithium could not be identified and was therefore also not included in the refinements. While an acceptable Rietveld fit has been realized for  $\text{Li}_{0.2}\text{CdP}_2$  (see Figure 4), a refinement was not possible for  $\alpha'$ - $\text{CdP}_2$ . The profile type changes from reflection to reflection in  $\text{CdP}_2$ , pointing towards severe strain formation during the de-lithiation and pronounced domain structure after the topotactic reaction.

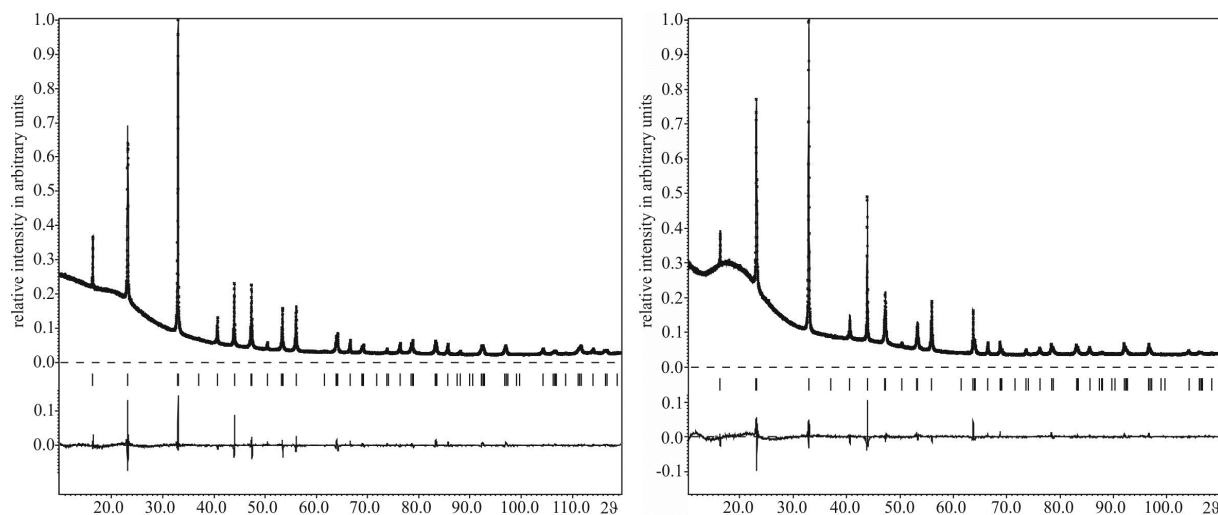


**Figure S11.** Rietveld refinement of  $\text{Li}_{0.2}\text{CdP}$  (left) and of  $\alpha'$ - $\text{CdP}_2$  (right). The structure model of  $\text{Li}_{0.2}\text{CdP}$  (only Cd and P sites) and  $\alpha'$ - $\text{CdP}_2$  has been taken from single crystal structure refinement. The experimental values are shown as crosses, the theoretical diagram superimposed as a line, below the Bragg positions as vertical lines. The lower line represents the difference  $I(\text{obs})-I(\text{calc})$ , with the reliability factors  $R_p = 2.84$ ,  $R_{wp} = 2.87$  and  $R(\text{all}) = 2.90$ ,  $R_w(\text{all}) = 2.87$  for  $\text{Li}_{0.2}\text{CdP}_2$  and  $R_p = 3.92$ ,  $R_{wp} = 4.19$  und  $R(\text{all}) = 4.19$ ,  $R_w(\text{all}) = 4.21$  for  $\text{CdP}_2$ .

A section of  $\alpha'$ - $\text{CdP}_2$  and  $\text{Li}_{0.2}\text{CdP}_2$  X-ray powder diffractograms at higher scattering angles is plotted in Figure S12 illustrating the very small differences between the two phases. Two general features must be discussed here, a peak shift to smaller  $2\theta$  values due to the slightly larger lattice parameters of  $\alpha'$ - $\text{CdP}_2$  and a significant enlargement of the reflection half-widths for  $\alpha'$ - $\text{CdP}_2$  in relation to  $\text{Li}_{0.2}\text{CdP}_2$ . The enlarged half-width is a direct consequence of the topotactic de-lithiation of  $\text{Li}_{0.2}\text{CdP}_2$ , resulting in much smaller crystal domains. This convolution is also a reason for the imperfect fits in the Rietveld refinements of both title compounds. It is highly possible that a fraction of  $\text{Li}_{0.2}\text{CdP}_2$  is delithiated either during the measurement or during the setup of the experiment.

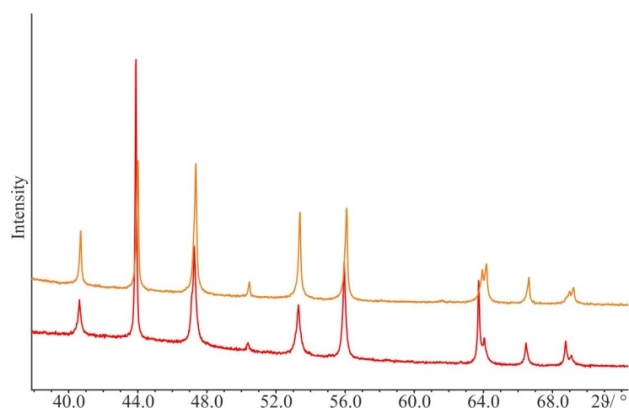


**Figure SI2.** X-ray powder diffraction of  $\text{Li}_{0.2}\text{CdP}_2$  (orange) and  $\alpha'$ - $\text{CdP}_2$  (red). A significantly larger half width of the  $\alpha'$ - $\text{CdP}_2$  reflections is obvious.

## 2. Verification of ICP results on $\text{Li}_{0.2}\text{CdP}_2$ and $\alpha'$ - $\text{CdP}_2$

Due to the fact that ICP showed a slightly lower Cd content ( $\text{Cd}_{0.889(5)}\text{P}_{2.00(1)}$  and  $\text{Li}_{0.199(3)}\text{Cd}_{0.895(5)}\text{P}_{2.00(2)}$ ) than expected ( $\text{CdP}_2$  and  $\text{Li}_{0.2}\text{CdP}_2$ ) we have tried to synthesize these compounds according the ICP results. We tried to prepare a charge balanced compound with the formal composition  $\text{Li}_{0.25}\text{Cd}_{0.875}\text{P}_2$ , a non-balanced  $\text{Li}_{0.2}\text{Cd}_{0.9}\text{P}_2$  and  $\text{Cd}_{0.9}\text{P}_2$ , including  $\text{CdI}_2$  as a mineralizer in all cases. The products  $\text{CdP}_4$ ,  $\text{Cd}_3\text{P}_2$  and  $\beta\text{-CdP}_2$  were found in X-ray powder diffraction experiments (see Figures SI2 and SI3). In no cases phase pure  $\alpha'$ - $\text{CdP}_2$  or  $\text{Li}_{0.2}\text{CdP}_2$  were detected.

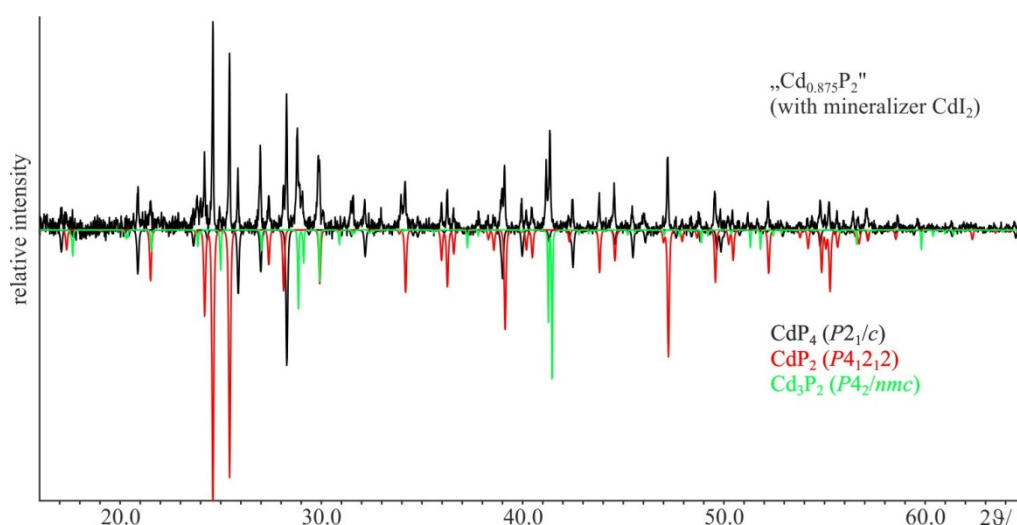


**Figure SI3.** Measured X-ray powder diffraction of a sample with the nominal composition of  $\text{Cd:P} = 0.875:2$  and  $\text{CdI}_2$  as mineralizer (black line at the top), at 295 K with  $\text{Cu-K}\alpha$ -radiation. The lines at the bottom are calculated X-ray powder diffraction pattern of  $\text{CdP}_4$  (black line),  $\text{CdP}_2$  (red line) and  $\text{Cd}_3\text{P}_2$  (green line).

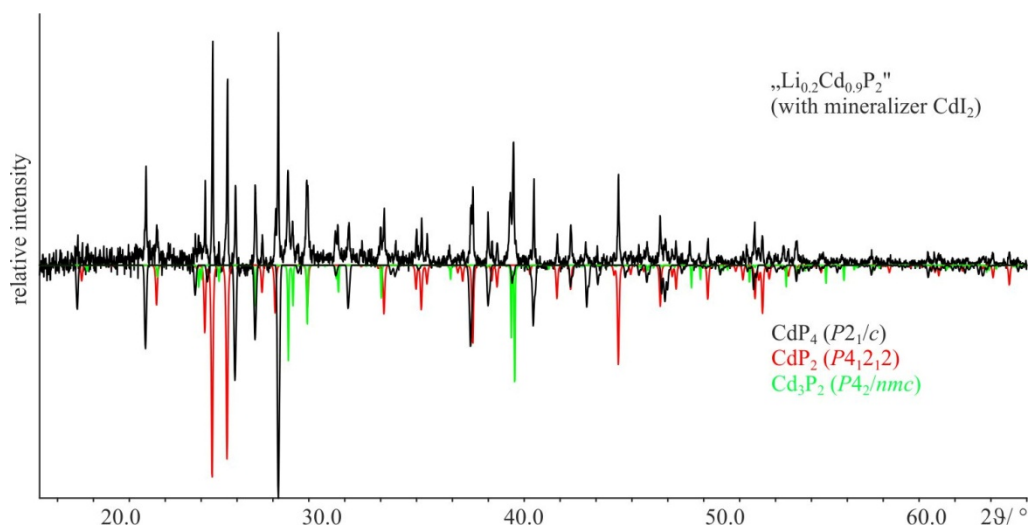


**Figure SI4.** Measured X-ray powder diffraction of the sample with the weighed portion of Li:Cd:P 0.2:0.9:2 and  $\text{CdI}_2$  as mineralizer (black line at the top) by 295 K with  $\text{Cu-K}\alpha$ -radiation. The lines at the bottom are calculated X-ray powder diffraction patterns of  $\text{CdP}_4$  (black line),  $\text{CdP}_2$  (red line) and  $\text{Cd}_3\text{P}_2$  (green line).

### 3. Analysis of the de-lithiation product of $\text{Li}_{0.2}\text{CdP}_2$

$\alpha'$ - $\text{CdP}_2$  can be prepared by a de-lithiation process from  $\text{Li}_{0.2}\text{CdP}_2$  crystals. After 24 h on air a white powder is formed on top of the needle-shaped crystals. The white powder is soluble in water. After dissolution and water removal on air  $\text{Li}_2\text{CO}_3$  was found as the main phase in the X-ray powder diffraction together with  $\text{Cd}(\text{P}_4\text{O}_{11})$ <sup>1</sup>.  $\text{Li}[\text{IO}_3]$ <sup>2</sup> and  $\text{Li}_2\text{O}$ <sup>3</sup> are possible additional side phases (see Figure SI3).

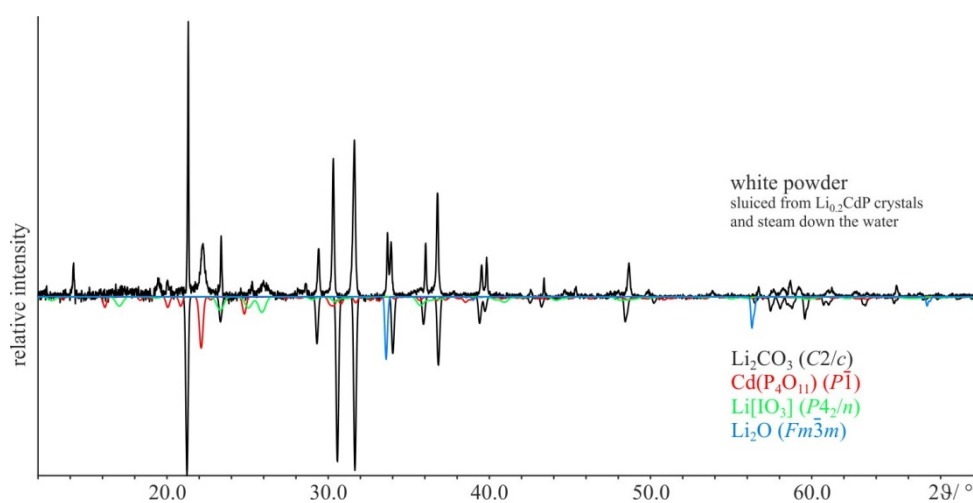


**Figure SI5.** Measured X-ray powder diffraction of white powder, slushed in water from  $\text{Li}_{0.2}\text{CdP}_2$  crystals and steam dried (black line at the top) by 295 K with  $\text{Cu-K}\alpha$ -radiation. The lines at the bottom are theoretical calculated X-ray powder diffraction patterns of  $\text{Li}_2\text{CO}_3$  (black line),  $\text{Cd}(\text{P}_4\text{O}_{11})$  [1] (red line),  $\text{Li}[\text{IO}_3]$  [2] (green line) and  $\text{Li}_2\text{O}$  [3] (blue line).

A semi quantitative EDX analysis of the white powder achieved after dissolving in water and evaporation of the solvent showed carbon 31(8) at-%, oxygen 62(8) at-%, phosphorus 6(1) at-% and iodine 2(1) at-%.

#### 4. DSC-Analysis of $\text{Li}_{0.2}\text{CdP}_2$

DSC measurement was performed with a Netzsch differential scanning calorimeter DSC 200 F3 at heating and cooling rates of  $10 \text{ K min}^{-1}$  in the temperature range between 120 and 360 K. Mercury, indium, tin, bismuth, zinc and caesium chloride were used for temperature calibration. Ground  $\text{Li}_{0.2}\text{CdP}_2$  crystals (14.2 mg) were measured under a constant nitrogen flow of  $50 \text{ ml min}^{-1}$  in sealed aluminium crucibles. There is no detectable DSC-effect in the measured range (see Figure SI6).

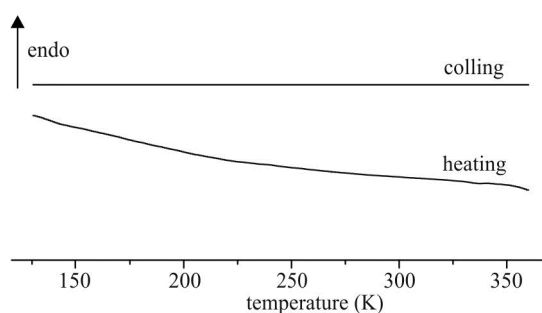


**Figure SI6.** DSC curves of  $\text{Li}_{0.2}\text{CdP}_2$  (temperature range 120-360 K).

#### 5. Conductivity measurements of $\text{Li}_{0.2}\text{CdP}_2$ and $\alpha'$ - $\text{CdP}_2$

The conductivity of powdered material was measured with a homemade tool, which is capable to measure powdered samples and applied pressure. The values of  $\text{Li}_{0.2}\text{CdP}_2$  ( $5.2 \times 10^{-5} \text{ S/cm}$ ) and  $\alpha'$ - $\text{CdP}_2$  ( $6.6 \times 10^{-9} \text{ S/cm}$ ) are not precise, nevertheless a tendency is discernible pointing towards a significantly enhanced conductivity in the case of the lithiated phase. Details concerning the experimental setup are given in the main text.

## 6. Quantum chemical calculations of $\text{Li}_{0.2}\text{CdP}_2$ and polymorphic $\text{CdP}_2$

As lithium is needed to stabilize  $\text{Li}_{0.2}\text{CdP}_2$  in space group  $I4_122$  ( $\alpha$ - $\text{CdAs}_2$  structure type) its role need to be clarified with the help of further DFT calculations. We intended to generate a structure model including Lithium occupying sense full positions. Therefore, the energies of the unit cells of both, with and without small amounts of Lithium are compared. Looking at the crystal structure of  $\alpha$ - $\text{CdAs}_2$ , there are basically two possible ways in which stabilizing lithium atoms can be inserted into the structure. The first possible structure option is a substitution of cadmium by lithium ions on  $4a$ . Based on ideal  $\text{CdP}_2$ , an eight fold super cell was generated ( $\text{Cd}_8\text{P}_{16}$ ) where one Cd is substituted by Li resulting in “ $\text{LiCd}_7\text{P}_{16}$ ” (space group  $P222$ , Figure SI7). A model for an intercalation of Li was constructed from  $\text{Cd}_8\text{P}_{16}$  by addition of one Li to the channels leading to “ $\text{LiCd}_8\text{P}_{16}$ ” (space group  $P2$ , Figure SI7). The intercalation of Li into channels, combined with a pronounced one dimensional mobility is most likely for  $\text{CdP}_2$  in the  $\alpha$ - $\text{CdAs}_2$  type (space group  $I4_122$ ). This could lead to a preferred formation of  $\alpha$ - $\text{CdAs}_2$  type  $\text{CdP}_2$ , rather than the known  $\alpha$ - and  $\beta$ - $\text{CdP}_2$  phases due to a stabilizing effect of Li ions within the empty channels in the  $\alpha$ - $\text{CdAs}_2$  type structure. From now on, we call the new  $\alpha$ - $\text{CdAs}_2$  type  $\text{CdP}_2$  polymorph  $\alpha'$ - $\text{CdP}_2$ . In good accordance with this assumption, LDA and GGA calculations illustrate that  $\alpha'$ - $\text{CdP}_2$  is destabilized compared with the lithiated phase. A rather small energy gain can be calculated for Li substitution and a significant energy gain for Li intercalation (Figure SI8, right hand side). LDA noticeably shifts  $\alpha'$ - $\text{CdP}_2$ , with Li intercalated in the empty channels, to an energy region of more than 2 kJ/mol per formula unit below known  $\alpha$ - and  $\beta$ - $\text{CdP}_2$ . This is a distinct piece of evidence that the incorporation of Li is a driving force for the formation of  $\text{Li}_{0.2}\text{CdP}_2$ . The results of the first principles calculations (0 K energies) of all  $\text{CdP}_2$  and  $\alpha$ - $\text{CdAs}_2$  polymorphs are denoted in Figure SI8. The title compound is highlighted with a yellow background and a dotted frame. For reasons of clarity, **the energy of  $\beta$ - $\text{CdP}_2$  is set as reference**. LDA calculations are presented in the upper part of the Figure, while GGA calculations are denoted at the bottom. Overall, there is good agreement of the calculated GGA/LDA energies with reported  $\alpha$ - $\text{CdAs}_2$  and  $\text{CdP}_2$  polymorphs. In most cases, the existing phases show low energies compared with non-existing ones.

Let us now focus on the stabilization effect by Lithium leading to the formation of  $\text{Li}_{0.2}\text{CdP}_2$ . LDA distinctly confirms the  $\alpha$ - $\text{CdAs}_2$  type phase as the most stable one featuring a distinct energy gain compared with all other  $\text{CdP}_2$  polymorphs. This trend can be explained by the

higher density of the new compound compared to the other structure types. It has to be mentioned that the LDA generally exhibits a tendency to prefer denser structures. On the other hand, stronger dispersive interactions between the pnictide helices, which the GGA does not sufficiently take into account, are expected for denser structures. A comparable but not that pronounced trend is also present in the GGA case. By all means, the LDA and the GGA calculations confirm that  $\alpha$ -CdAs<sub>2</sub> type Li<sub>0.2</sub>CdP<sub>2</sub> is stabilized due to the Li intercalation.

$\alpha'$ -CdP<sub>2</sub>, the de-lithiated form of Li<sub>0.2</sub>CdP<sub>2</sub>, possesses the  $\alpha$ -CdAs<sub>2</sub> structure type. Our calculations show that  $\alpha'$ -CdP<sub>2</sub> must be metastable in relation to  $\alpha$ -CdP<sub>2</sub>.

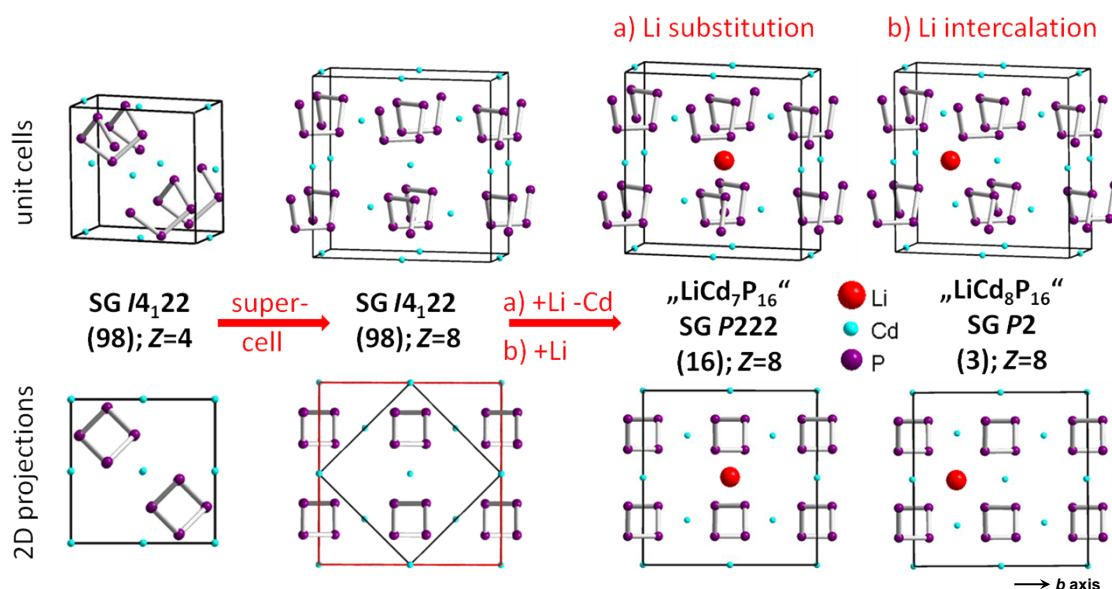


**Figure SI7.** Two different views (rows) for CdP<sub>2</sub>, adopting the  $\alpha$ -CdAs<sub>2</sub> structure type, illustrating the applied super cell approach to model the insertion of Li. After the enlargement of the unit cell Lithium is either placed on a Cd site or within the empty channels (from left to right). P (pink spheres), Cd (cyan, small spheres) and Li (red, large spheres).

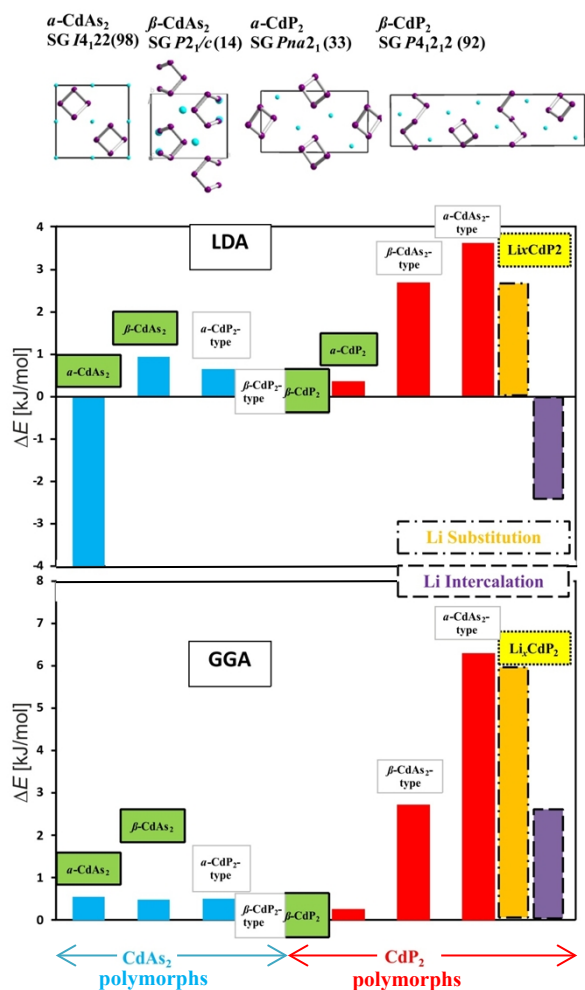


**Figure SI8.** Bar diagram featuring energy differences (relative to  $\beta$ -CdP<sub>2</sub> or  $\beta$ -CdAs<sub>2</sub> which were set as reference) between different modifications of CdAs<sub>2</sub> and CdP<sub>2</sub>. The experimentally known modifications are highlighted in green in the name box. Hypothetic polymorphs are kept white. For  $\alpha'$ -CdP<sub>2</sub>, the two possible structure models featuring lithium substitution (orange) and intercalation (purple) in space group  $I4_122$  are shown on the right hand side. Known compounds are given together with their structures in the upper part of the figure.

### 7. Quantification of proton content with <sup>1</sup>H-MAS-NMR in $\alpha'$ -CdP<sub>2</sub>

The amount of protons in  $\alpha'$ -CdP<sub>2</sub> was estimated as follows. Using mixtures of BaHPO<sub>4</sub>/SiO<sub>2</sub> and Na<sub>2</sub>H<sub>2</sub>P<sub>2</sub>O<sub>7</sub>/SiO<sub>2</sub> and measuring the observed signal intensity of the <sup>1</sup>H-MAS NMR spectra (The spectra were acquired at a rotation frequency of 30 kHz; the background signal

was subtracted and the  $\pi/2$  pulse lengths were carefully optimized for each experiment,) a calibration curve was generated (cf. Fig. SI9).

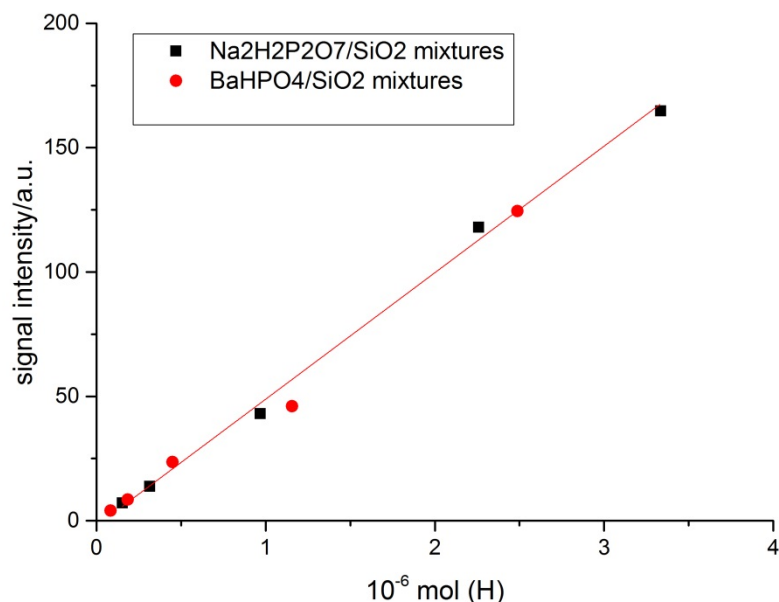


**Figure SI9.**  $^1\text{H}$ -MAS NMR signal intensity plotted against the sample proton quantity for different mixtures. This correlation was used as a calibration curve for the determination of the proton content in  $\alpha'$ - $\text{CdP}_2$ .

Then, the corresponding signal intensities for three different samples of in  $\alpha'$ - $\text{CdP}_2$  was determined and the number of protons evaluated. From this, we conclude a proton content according to  $\text{H}_{0.050(5)}\text{CdP}_2$ . Although this approach only allows for a rough estimation of the proton content (cf. cit. 4), this result clearly disfavours any stoichiometric proton exchange during the reaction.

## References

- (1). M. Weil, R. Glaum, *Eur. J. Solid State Inorg. Chem.* **1998**, 35, 495-508.
- (2). H. Schulz, *Acta Crystallogr. B* **1973**, 29, 2285-2289.
- (3). E. Zintl, A. Harder, B. Dauth, *Z. Elektrochem. Angew. Phys. Chem.* **1934**, 40, 588-593.
- (4). Y. S. Avadhut, D. Schneider, J. Schmedt auf der Günne, *J. Magn. Reson.* **2009**, 201, 1.